神経幹細胞移植（細胞数 $1x10^6$個）を損傷部に行った。損傷後 10 週まで QSI を全麻下で撮像した。QSI の評価は myelin map を用いて行い、その後灌流固定し組織学的所見と比較検討した。

C．研究結果

1）正常サル脊髄の QSI

生きているサルの脊髄の明瞭な QSI の描出に成功した。displacement、zero displacement、kurtosis の各パラメーターを検討した結果、displacement map の信号強度は組織の大きさを反映し、Kurtosis の信号は組織の密度を反映していた。

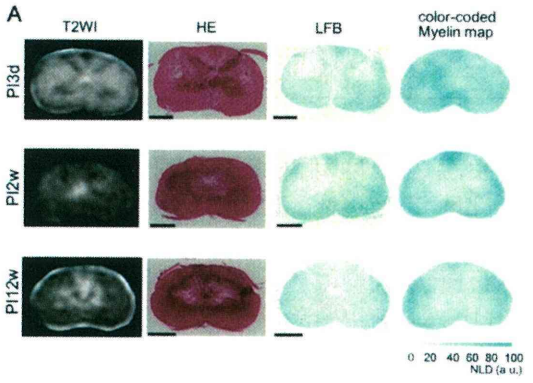

図１

2）サル損傷脊髄の QSI

3 つのパラメーターを用いて損傷脊髄内の信号値を算出し、HE 染色と LFB 染色による残存髄鞘面積との比較検討の結果、従来の T2WI ではとらえることができなかった組織学的な変化（空洞形成、細胞脱落、脱髄）を displacement map, kurtosis は反映していた（図１）。

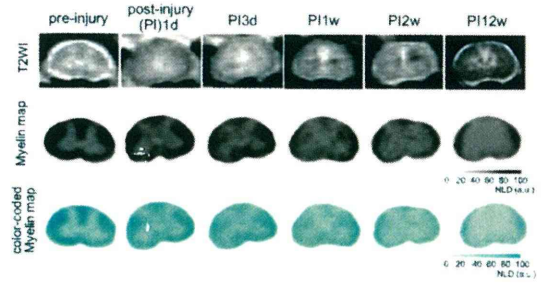

図２

次に同一個体において脊髄損傷後の脊髄内信号強度の経時的な変化を検討し、損傷後白質内の髄鞘と kurtosis の信号値を応用し独自に開発した Myelin map は、LFB 陽性の残余髄鞘領域を明瞭に示していた（図２）。

3）サル損傷脊髄に対するサル胎児由来神経幹細胞後の QSI による髄鞘の可視化

最後にサル損傷脊髄に対するサル胎児由来神経幹細胞移植の効果を髄鞘に着目して、QSI により評価ができるか否かを検討した。培養サル神経幹細胞は、分化誘導を行うと神経 3 系統へと分化した。サル神経幹細胞移植後の myelin map では、損傷脊髄内で脱髄が進行し、その後再髄鞘化が起こることを myelin map でとらえることに成功した（図３）。また、これらの所見は LFB 染色と免疫電顕でも確認できた（図４）。

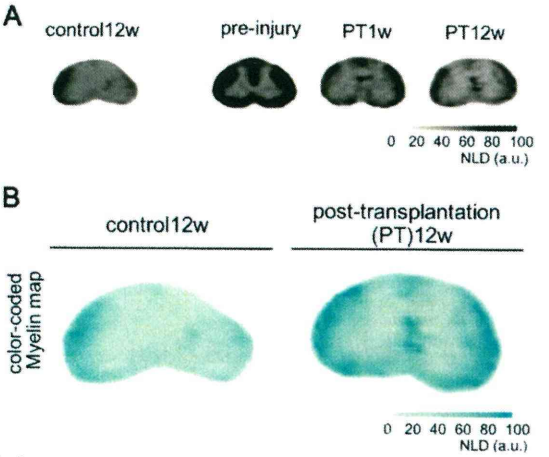

図３

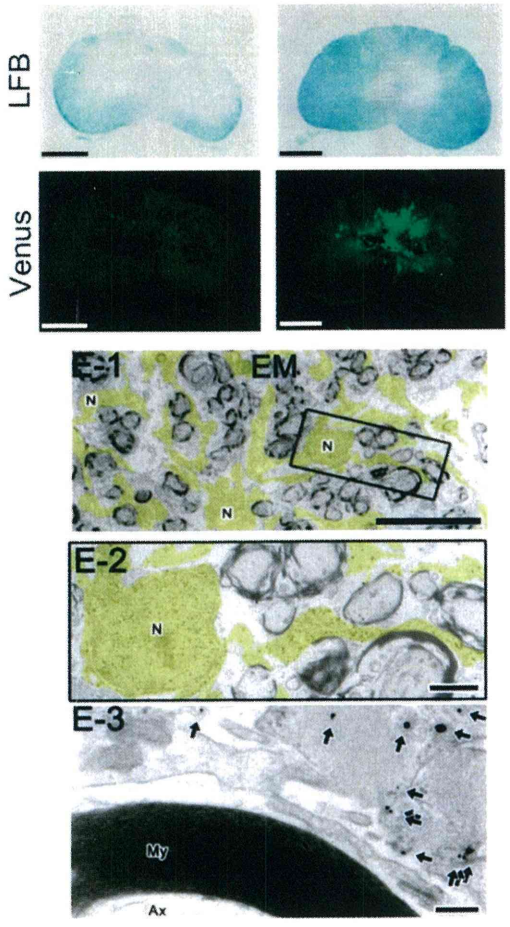

図４

D．考察

我々は QSI のパラメーターの中で kurtosis が最も鋭敏に水分子の制限を検出することを発見し、これを応用して髄鞘の可視化法である“Myelin map”の開発に成功した。Myelin map により従来組織学的に評価せざるを得なかった損傷脊髄内の脱髄変化を、非侵襲的かつ定量的に評価できることが明らかとなった。

MRI は非侵襲的に生体内部構造を観察できる方法であるが、従来の T1/T2 強調像のみから脊髄損傷の重症度や機能的予後を正確に予測することは困難であった。脊髄損傷による軸索の断裂や神経細胞死、それに続いて起こる脱髄、空洞やグリア瘢痕形成等の変化のうち、残余髄鞘面積が運動機能と相関があることを既に我々は報告した（Iwanami et al. JNR 2005)。今回の検討より、１）髄鞘可視化技術である Myelin map によって動物を生かしたままで脊髄内の髄鞘の変化を定量的に評価できる、２）脊髄損傷後の比較的早期に残余髄鞘を定量的に捉えることにより、機能的予後を早期に予測することできる可能性が示唆され、今後の脊髄再生医療における脊髄損傷後の重症度判定あるいは種々の治療法の効果判定における強力な評価法となりうると考えている。

E．結論

QSI による脊髄内髄鞘の可視化に世界で初めて成功した。われわれはこの方法を Myelin map として提唱したい。Myelin map は脊髄損傷の診断は勿論のこと、将来計画している肝細胞増殖因子を用いた中枢神経の再生医療の治療効果判定に大きく役立つものと考えている。

F．健康危険情報

特になし

G．研究発表

1. 論文発表

なし

2. 学会発表

藤吉兼浩、疋島啓吾、北村和也、辻収彦、岡野栄之、戸山芳昭、中村雅也：拡散テンソルトラクトグラフィーによる霊長類脊髄圧挫損傷の in vivo imaging　第 38 回日本脊椎脊髄病学会　2009.4.24

Fujiyoshi Y, Nakamura M, et al: q-space MR imaging depict demyelination after spinal cord injury in non-human primate. Annual meeting of neuroscience Chicago, USA 2009.10.20

藤吉兼浩、岡野栄之、中村雅也ほか：q-space imagingを用いた脊髄再生メカニズムの解明 ～再生医療への応用～第37回日本磁気共鳴医学会大会　2009.10.1 横浜

藤吉兼浩、岡野栄之、中村雅也ほか：q-space imagingを用いた脊髄損傷における脱髄評価　第24回日本整形外科学会基礎学術集会　2009.11.5　横浜

許斐恒彦, 岡野栄之, 中村雅也ほか in vivo QSI を用いた霊長類脊髄損傷モデルにおける損傷強度別経時的 Myelin map. 第25回日本整形外科学会基礎学術集会, 2010.10.14　京都

Konomi T, Nakamura M, Okano H, et al. Myelin map after graded spinal cord injury in adult common marmosets. 40th Annual meeting Neuroscience 2010, San Diego, CA, USA

H. 知的財産権の出願・登録状況

1. 特許取得
　なし
2. 実用新案登録
　なし
3. その他
　なし

厚生労働科学研究費補助金（難治性疾患克服研究事業）
分担研究報告書

「肝細胞増殖因子による筋萎縮性側索硬化症に対する新規治療法の開発」
－非臨床試験、治験薬製造、臨床試験の実施－

研究分担者：　安達　喜一（クリングルファーマ株式会社 事業開発部長）
共同研究者：　阿部　哲士（クリングルファーマ株式会社 医薬開発部長）
福田　一弘（クリングルファーマ株式会社 研究開発部長）
井上　逸男（クリングルファーマ株式会社 品質保証部長）

研究要旨

肝細胞増殖因子（HGF）は、筋萎縮性側索硬化症（ALS）のモデル動物（マウス、ラット）において運動ニューロン保護、生存延長効果をもつことが報告されている。多くの神経栄養因子の中でも、この様に変異 SOD1 トランスジェニック動物による ALS モデルに対して明確な治療効果を示したものは少なく、この有効性を ALS 患者に臨床応用する意義と必要性がある。ALS を対象とする HGF の臨床試験実施に向けて、カニクイザルによる非臨床試験（GLP 毒性試験および薬物動態試験）を行い、脊髄腔内投与による HGF の安全性と薬物動態を確認した。これらの結果に基づいて第Ⅰ相臨床試験の用量・用法を設定した。一方、脊髄腔内投与用の製剤化検討を行い、第Ⅰ相臨床試験で用いる治験薬を製造すると共に、治験薬（液剤および希釈液）の安定性試験を開始した。さらに、第Ⅱ相臨床試験以降に使用する新規の凍結乾燥製剤を開発した。第Ⅰ相臨床試験の準備は、プロトコール開発からプロジェクトマネジメント、モニタリング・監査・統計解析・データマネジメント、治験コーディネーター（CRC）育成に至るまで東北大学トランスレーショナルリサーチ（TR）センターの全面的支援を得て進めた。平成 23 年 6 月に第Ⅰ相臨床試験の治験届を医薬品医療機器総合機構（PMDA）に、同年 7 月に東北大学病院治験審査委員会（IRB）に提出し承認を得た。現在、東北大学病院において第Ⅰ相臨床試験を実施中である。

A．研究目的

本研究の目的は、肝細胞増殖因子（HGF）の筋萎縮性側索硬化症（ALS）に対する第Ⅰ相臨床試験を実施し、脊髄腔内投与による安全性と薬物動態を確認することである。平成 21 年度および 22 年度に、臨床試験を開始するために必要となる非臨床試験、治験薬製造、プロトコール作成を行った。平成 23 年度は、前年度までの準備を踏まえて第Ⅰ相臨床試験を開始することを主目標とし、併せて治験薬の安定性試験と原薬製造ならびに凍結乾燥製剤の開発を行った。

B．研究方法

1）カニクイザルによる非臨床試験（GLP 毒性試験および薬物動態試験）

臨床応用の最も可能性の高いルートとしての髄腔内投与での効果が ALS ラットで確認されたことから、カニクイザルに対する髄腔内投与による安全性試験を GLP 基準で行った。すなわち、ヒト

組換えHGF蛋白質（3用量）をカニクイザル（各群雄4匹）の脊髄腔内に4週間持続投与したときの毒性変化を調べるとともに、4週間の休薬期間を設けてその回復性について検討した。また、そのときの全身的曝露についても評価した。本試験は、①髄腔内持続投与の安全性と同時に、②髄腔内投与時の薬物動態（HGFの髄腔内分布・排泄経路の確認、全身への移行性など）を確認することを目的とする。

2) 治験薬製造

ヒト組換えHGF蛋白質製剤としては、すでに臨床試験で使用実績のある静注用製剤があるが、組成の中に髄腔内投与の使用実績のない、あるいは使用実績を超える賦形剤が含まれている。従って、安全性を考慮し、髄腔内投与用に製剤組成を変更することにした。新たに製剤（液剤）化の試作検討を行い、既存の髄注製剤の使用実績を超えない範囲で賦形剤の組成を決定した。第Ⅰ相臨床試験に使用する注射液剤と投与濃度に希釈するための希釈液を、GMP基準で製造した。また、HGF製剤の試作品を用いて予備安定性試験を開始した。

第Ⅱ相臨床試験で使用する凍結乾燥製剤を新たに開発するために必要となるHGFの原薬製造を行った。HGF産生細胞のマスターセルバンク（MCB）から作製したワーキングセルバンク（WCB）を用いて培養を開始し、培養スケールを拡大した。拡大培養終了後、細胞をろ過除去し、培養上清を得た。培養上清中に含まれる不活性な一本鎖HGFを活性型の二本鎖HGFに変換した後、精製工程に移行した。精製工程では多段階のカラムクロマトグラフィーによりHGFを精製した。上記の製造はすべてGMP基準で実施した。製造したHGF原薬は、品質標準書に従って規格試験を実施し、それらの結果に基づいて出荷の可否を判定した。製造したHGF原薬を用いて凍結乾燥製剤の開発に着手した。

3) 第Ⅰ相臨床試験

東北大学TRセンターの全面的支援を得て、第Ⅰ相臨床試験の準備、すなわちプロトコール開発、プロジェクトマネジメント、モニタリング・監査・統計解析・データマネジメント、CRC育成を行った。また、臨床試験において必要となるヒト血漿および髄液中のHGFおよび抗HGF抗体の定量検査の委託先、ならびにモニタリングおよび監査を担当する開発業務受託機関（CRO）を選定した。医薬品・医療機器総合機構（PMDA）との対面助言（治験開始前相談）を経て、治験届をPMDAならびに東北大学病院治験審査委員会（IRB）に提出し治験を開始した。

C．研究結果

1) カニクイザルによる非臨床試験（GLP毒性試験および薬物動態試験）

GLP基準によるカニクイザルに対する髄腔内投与による安全性試験を行った。平成21年度に施行した予備試験の結果を受け、平成22年度に本試験を実施・完了した。投与および休薬期間中、死亡例はみられなかった。また、一般状態、一般症状および神経行動学的機能観察では、いずれの群においてもHGFに起因すると考えられる変化は認められなかった。病理組織学的検査では、臨床用量の60倍を超える高用量群においても毒性所見は認められなかった。本試験において、①髄腔内持続投与の安全性ならびに、②髄腔内投与時の薬物動態の確認

（HGF の髄腔内分布・排泄経路の確認、全身への移行性など）を確認することができた。

2) 治験薬製造

第Ⅰ相臨床試験に使用する治験薬（注射液剤）と希釈液を GMP 基準で製造した。製造工程において異常は認められず、製造標準書どおりに製造することができた。製造した注射液剤と希釈液について規格試験を実施したところ、すべての規格に適合し、出荷可否判定において合格と判定された。また、安定性試験を平成 23 年度まで継続し、液剤は 18 ヶ月点まで、希釈液は 6 ヶ月点までの安定であることを確認し、治験に使用する上で安定性に問題がないことを確認した。

現行の凍結溶液製剤（液剤）に変わる新製剤を検討するための原薬を製造した。培養工程および精製工程のいずれにおいても異常は認められず、製造標準書通りに HGF 原薬を製造することができた。製造した HGF 原薬はすべての規格試験に適合した。製造した原薬を用いて新製剤を開発した。新製剤は凍結乾燥製剤であり、現行の凍結溶液製剤に比べて扱いやすく、今後の第Ⅱ相試験から使用する予定である。

3) 第Ⅰ相臨床試験

第Ⅰ相臨床試験の準備は、東北大学病院を実施医療機関とし（治験責任医師：神経内科 青木正志）、東北大学 TR センター（未来医工学治療開発センター）各部門の支援の下で行った。東北大学 TR センター審査・評価部門と協同し、第Ⅰ相臨床試験のプロトコール、ならびに治験必須文書（治験薬概要書、治験機器概要書、治験実施計画書、患者同意説明文書、症例報告書）および各種手順書を作成した。第Ⅰ相臨床試験のプロトコールの策定にあたっては、平成 22 年度までに実施した薬物動態試験および毒性試験の結果に基づいて、用量・投与間隔などを設定した。また、治験としての安全性や倫理的妥当性を薬事法および GCP に遵守して確保するために、東北大学 TR センター検証・情報管理部門の支援を受けてモニタリング・監査・統計解析・データマネジメントの整備も進めた。また、東北大学 TR センター教育・人材育成部門において CRC の育成を行うと同時に、担当モニター（シミック）を交えての各種手順の確認を行い、GCP に沿った治験実施体制を整えた。全体のプロジェクトマネジメントは東北大学 TR センター審査・評価部門にて行った。

一方、臨床試験で使用する投与機器として、カテーテルと皮下ポートのセットとなっているポータカットⅡ（スミスメディカル）を選定した。ポータカットⅡを使用することにより、皮下ポートを介して HGF を髄腔内に繰り返し投与することが可能となった。また、臨床試験の薬物動態等の検査施設として新日本科学を、CRO としてシミックを選定した。

以上のように構築した第Ⅰ相臨床試験の実施体制を下図に示す。

第Ⅰ相臨床試験の実施体制

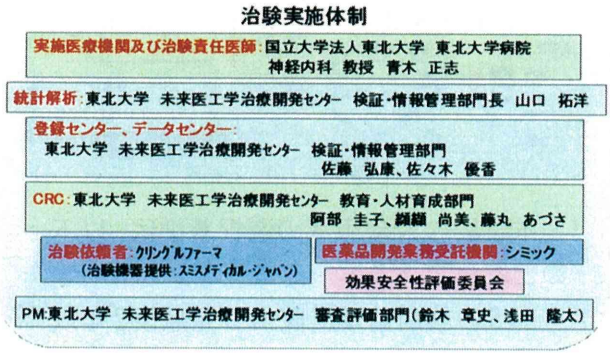

上記の準備を経て、平成 23 年 6 月に第 I 相臨床試験の治験届を医薬品医療機器総合機構（PMDA）に、同年 7 月に東北大学病院 IRB に提出し其々承認を得た後、第 I 相臨床試験を開始した。本試験は ALS 患者を対象とし、HGF を髄腔内投与したときの安全性・忍容性および薬物動態を確認することを目的とする。本試験では、ALS で障害を受ける脊髄神経に直接 HGF を作用させることを狙っており、このため、髄腔内に直接 HGF を投与する。HGF の髄腔内投与のためには、専用のカテーテルを髄腔に埋め込むこととする。本試験はオープンラベルで行い、用量漸増（低、中、高用量）による髄腔内単回投与と、安全性を確認した最高用量での髄腔内反復投与の計 4 群（12 例）の試験である。各群終了時に外部医学専門家で構成する効果安全性評価委員会による臨床評価を行い、安全性には十分配慮して試験を進めることとした。なお、東北大学 TR センター臨床応用部門より、効果安全性評価委員会の委員に加わって頂いた。第 I 相臨床試験の概要を下図に示す。

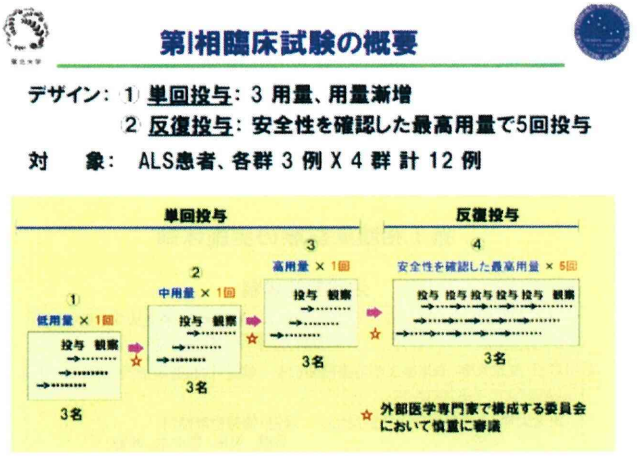

本試験の対象患者の選択基準は、以下のとおりである。

- ALS の診断基準に該当し発症後 2 年以内
- ALS の重症度分類が 1 もしくは 2
- 年齢が 20 歳以上、65 歳未満
- 投与・観察期間の一定期間の入院が可能
- 治験参加に同意

また、ALS 以外の重篤な疾患がある方、癌あるいは癌の既往のある方、医療機器にアレルギーのある方などは本試験から除外することとした。

平成 24 年 2 月 14 日現在、1 例目の被験者（単回投与・低用量群）への投与が終了し、経過観察を行っているが、特段の副作用は観察されていない。1 例目被験者の観察終了を待って、2 例目被験者の組み入れ（3 月中）を予定している。

D．考察

平成 21 年度および 22 年度までの非臨床試験、製剤検討、プロトコール策定および治験体制の構築を経て、平成 23 年度は、主目標であった第 I 相臨床試験を開始することができた。平成 24 年度以降、投与症例数を重ねて本試験を完了し、HGF の髄腔内投与による安全性・忍容性および薬物動態に関する臨床データを取得する。また、本試験終了後、引き続いて ALS 患者での有効性を確認するための第 II 相臨床試験（いわゆる Proof of Concept 試験；POC 試験）を実施する予定である。第 II 相臨床試験では、HGF を髄腔内に長期投与することを計画している。よって、長期投与の安全性を担保するために、カニクイザルによる慢性毒性試験を GLP 準拠で実施する必要がある。平成 24 年度以降、第 I 相臨床試験と並行して上記非臨床試験を実施する予定である。

治験薬の製造関係では、平成 23 年度に製造した HGF 原薬を用いて凍結乾燥製剤の処方を各種検討した結果、最適な

凍結乾燥製剤の開発に成功した（下写真）。第Ⅱ相臨床試験ではより扱いやすい凍結乾燥製剤の治験薬に変更することが可能である。

E．結論

HGF の ALS に対する第Ⅰ相臨床試験を開始するために必要な、非臨床試験および治験薬製造を実施・完了した。東北大学 TR センターの全面的な支援を得て第Ⅰ相臨床試験の準備を行った。PMDA および治験施設 IRB から治験届の承認を得て、東北大学病院において ALS 患者を対象とする第Ⅰ相臨床試験を開始した。1 例目の被験者に HGF の投与を終了し、経過観察中であるが、特段の副作用は観察されていない。

第Ⅰ相臨床試験は今後も継続するが、使用する治験薬（液剤および希釈液）の安定性試験の結果、以後の試験継続中も十分な安定を有していることを確認した。また、今後の第Ⅱ相試験で使用する、より扱いやすい凍結乾燥製剤の開発にも成功した。

第Ⅰ相試験を終了した後は、すみやかに第Ⅱ相試験に移行できる体制にあると考えられる。

F．健康危険情報

特記なし。

G．研究発表

1. 論文発表
   なし。

2. 学会発表
   なし。

H．知的財産権の出願・登録状況

1. 特許取得
   なし。

2. 実用新案登録
   なし。

3. その他
   なし。

研　究　成　果　の　刊　行

研究成果の刊行に関する一覧

書籍

著者	論文タイトル	書籍全体の編集者	書籍名	出版社	頁	出版年
船越 洋	神経栄養因子・再生因子による神経疾患の疾患進行・再生の分子機構の解析と適用	伊藤 正男・川合 述史	ブレインサイエンス・レビュー 2010	クバプロ（財）ブレインサイエンス振興財団	95-113	2010

原著論文

著者	論文タイトル	掲載誌名	巻 頁	出版年
Kadoyama K, Funakoshi H, Ohya-Shimada W, Nakamura T, Matsumoto K, Matsuyama S, Nakamura T	Disease-dependent reciprocal phosphorylation of serine and tyrosine residues of c-Met/HGF receptor contributes disease retardation of a transgenic mouse model of ALS.	Neurosci Res	65(2) 194-200	2009
Tanaka S, Miyata T, Fujita T, Kawahara E, Tachino K, Funakoshi H, Nakamura T	Differing responses of satellite cell activity to exercise training in rat skeletal muscle.	J. Phys. Ther. Sci	21 141-145	2009
Kanai M, Nakamura T, Funakoshi H	Identification and characterization of novel variants of the tryptophan 2,3-dioxygenase gene: differential regulation in the mouse nervous system during development.	Neurosci Res	64(1) 111-117	2009
Kanai M, Funakoshi H, Takahashi H, Hayakawa T, Mizuno S, Matsumoto K, Nakamura T	Tryptophan 2,3-dioxygenase is a key modulator of physiological neurogenesis and anxiety-related behavior in mice.	Mol Brain	2(1) 8	2009
Hocking JC, Hehr CL, Bertolesi G, Funakoshi H, Nakamura T, McFarlane S	LIMK1 acts downstream of BMP signaling in developing retinal ganglion cell axons but not dendrites.	Dev. Biol	330(2) 273-285	2009
Benkhoucha M, Santiago-Rabera ML, Schneitera G, Chofflon M, Funakoshi H, Nakamura T, . Lalive PH	Hepatocyte growth factor inhibits CNS autoimmunity by inducing tolerogenic dendritic cells and CD25+Foxp3+ regulatory T cells.	Proc Natl Natl Acad Sci USA	107(14) 6424-6429	2010
Mukaino M, Nakamura M, Yamada O, Okada S, Morikawa S, Renault-Mihara F, Iwanami A, Ikegami T, Ohsugi Y, Tsuji O, Katoh H, Matsuzaki Y, Toyama Y, Liu M, Okano H	Anti-IL-6-receptor antibody promotes repair of spinal cord injury by inducing microglia-dominant inflammation.	Exp Neurol	224(2) 403-414	2010
Tsuji O, Miura K, Okada Y, Fujiyoshi K, Mukaino M, Nagoshi N, Kitamura K, Kumagai G,Nishino M,Tomisato S,Higashi H, Nagai T, Katoh H, Kohda K, Matsuzaki Y, Yuzaki M, Ikeda E, Toyama Y, Nakamura M, Yamanaka S, Okano H	Therapeutic potential of appropriately evaluated 'safe' induced pluripotent stem cells for spinal cord injury.	Pro Nat Acad Sci USA	13:107(28) 12704-12709	2010
Shang J, Deguchi K, Yamashita T, Ohta Y, Zhang H, Morimoto N, Liu N, Zhang X, Tian F, Matsuura T, Funakoshi H, Nakamura T, and Abe K	Antiapoptotic and Antiautophagic Effects of Glial Cell Line-Derived Neurotrophic Fector and Hepatocyte Growth Factor After Transient Middle Cerebral Artery Occlusion in Rats.	J Neurosci Res	88(10) 2197-206	2010
Suzuki N, Aoki M, Warita H, Kato M, Mizuno H, Shimakura N, Akiyama T, Furuya H, Hokonohara T, Iwaki A, Togashi S, Konno H, Itoyama Y	FALS with FUS mutation in Japan with early onset, rapid progress and basophilic inclusion.	J Hum Genet	55 252-254	2010
Hadano S, Otomo A, Kunita R, Suzuki-Utsunomiya K, Akatsuka A, Koike M, Aoki M, Uchiyama Y, Itoyama Y, Ikeda JE	Loss of ALS2/Alsin exacerbates motor dysfunction in a SOD1H46R-expressing mouse ALS model by disturbing endolysosomal trafficking.	PLoS ONE	5(3) e9805	2010
Suzuki N, Takahashi T, Aoki M, Misu T, Konohana S, Okumura T, Takahashi H, Kameya S, Yamaki K, Kumagai T, Fujihara K, Itoyama Y	Neuromyelitis optica preceded by hyperCKemia episode.	Neurology	74 1543-5	2010
Maruyama H, Morino H, Ito H, Izumi Y, Kato H, Watanabe Y, Kinoshita Y, Kamada M, Nodera H, Suzuki H, Komure O, Matsuura S, Kobatake K, Morimoto N, Abe K, Suzuki N, Aoki M, Kawata A, Hirai T, Kato T, Ogasawara K, Hirano A, Takumi T, Kusaka H, Hagiwara K, Kaji R, Kawakami H	Mutations of optineurin in amyotrophic lateral sclerosis.	Nature	465 223-6	2010

Kobayashi Z, Tsuchiya K, Arai T, Aoki M, Hasegawa M, Ishizu H, Akiyama H, Mizusawa H	Occurrence of basophilic inclusions and FUS-immunoreactive neuronal and glial inclusions in a case of familial amyotrophic lateral sclerosis.	J Neurol Sci	293 6-11	2010
Suzuki N, Mizuno H, Warita H, Takeda S, Itoyama Y, Aoki M	Neuronal NOS is dislocated during muscle atrophy in amyotrophic lateral sclerosis.	J Neurol Sci	294 95-101	2010
Sanagi T, Yuasa S, Nakamura Y, Suzuki E, Aoki M, Warita H, Itoyama Y, Uchino S, Kohsaka S, Ohsawa K	Appearance of phagocytic microglia adjacent to motoneurons in spinal cord tissue from a presymptomatic transgenic rat model of amyotrophic lateral sclerosis.	J Neurosci Res	88 2736-46	2010
Katsuno M, Banno H, Suzuki K, Takeuchi Y, Kawashima K, Yabe I, Sasaki H, Aoki M, Morita M, Nakano I, Kanai K, Ito S, Ishikawa K, Mizusawa H, Yamamoto T, Tsuji S, Hasegawa K, Shimohata T, Nishizawa M, Miyajima H, Kanda F, Watanabe Y, Nakashima K, Tsujino A, Yamashita T, Uchino M, Fujimoto Y, Tanaka F, Sobue G	Efficacy and safety of leuprorelin in patients with spinal and bulbar muscular atrophy (JASMITT study): a multicentre, randomised, double-blind, placebo-controlled trial.	Lancet Neurol	9 875-884	2010
Shimazawa M, Tanaka H, Ito Y, Morimoto N, Tsuruma K, Kadokura M, Tamura S, Inoue T, Yamada M, Takahashi H, Warita H, Aoki M, Hara H	An inducer of VGF protects cells against ER stress-induced cell death and prolongs survival in the mutant SOD1 animal models of familial ALS.	PLoS ONE	5(12) e15307	2010
Takahashi Y, Tsuji O, Kumagai G, Miyauchi HC, Okano HJ, Miyawaki A,Toyama Y, Okano H, Nakamura M	Comparative study of methods for administering neural stem/progenitor cells to treat spinal cord injury in mice.	Cell Transplant	20(5) 727-739(13)	2011
Ito H, Fujita K, Nakamura M, Wate R, Kaneko S, Sasaki S, Yamane K, Suzuki N, Aoki M, Shibata N, Togashi S, Kawata A, Mochizuki Y, Mizutani T, Maruyama H, Hirano A, Takahashi R, Kawakami H, Kusaka H	Optineurin is co-localized with FUS in basophilic inclusions of ALS with FUS mutation and in basophilic inclusion body disease.	Acta Neuropathol	121(4) 555-557	2011
Iida A, Takahashi A, Kubo M, Saito S, Hosono N, Ohnishi Y, Kiyotani K, Mushiroda T, Nakajima M, Ozaki K, Tanaka T, Tsunoda T, Oshima S, Sano M, Kamei T, Tokuda T, Aoki M, Hasegawa K, Mizoguchi K, Morita M, Takahashi Y, Katsuno M, Atsuta N, Watanabe H, Tanaka F, Kaji R, Nakano I, Kamatani N, Tsuji S, Sobue G, Nakamura Y, Ikegawa S	A functional variant in ZNF512B is associated with susceptibility to amyotrophic lateral sclerosis in Japanese.	Hum Mol Genet	20(18) 3684-3692	2011
Suzuki N, Akiyama T, Takahashi T, Komuro H, Warita H, Tateyama M, Itoyama Y, Aoki M	Continuous administration of poloxamer 188 reduces overload-induced muscular atrophy in dysferlin-deficient SJL mice.	Neurosci Res	in press	2011
Aoki M, Warita H, Mizuno H, Suzuki N, Yuki S, Itoyama Y	Feasibility study for functional test battery of SOD transgenic rat (H46R) and evaluation of edaravone, a free radical scavenger.	Brain Res	1382 321-325	2011
Kitamura K, Fujiyoshi K, Yamane J, Toyota F, Hikishima K, Nomura T, Funakoshi H, Nakamura T, Aoki M, Toyama Y, Okano H, Nakamura M	Human hepatocyte growth factor promotes functional recovery in primates after spinal cord injury.	PLoS One	6(11) e27706	2011
Takagi T, Ishii K, Shibata S, Yasuda A, Sato M, Nagoshi N, Saito H, Okano HJ, Toyama Y, Okano H, Nakamura M	Schwann-Spheres Derived from Injured Peripheral Nerves in Adult Mice -Their In Vitro Characterization and Therapeutic Potential.	PLoS ONE PLoS One	6(6) e21497	2011
Renault-Mihara F, Katoh H, Ikegami T, Iwanami A, Mukaino M, YAasuda, Nori S, Mabuchi Y, Tada H, Shibata S, Saito K, Matsushita M, Kaibuchi K, Okada S, Toyama Y, Nakamura M,Okano H	Beneficial compaction of spinal cord lesion by migrating astrocytes through glycogen synthase kinase-3 inhibition.	EMBO Molecular Medicine	3(11) 682-696	2011
Yasuda A, Tsuji O, Shibata S, Nori S, Takano M, Kobayashi Y, Takahashi Y, Fujiyoshi K, Miyauchi Hara C, Miyawaki A, Okano JH, Toyama Y, Nakamura M, Okano H	Significance of Re-myelination by Neural Stem/Progenitor Cells Transplanted Into the Injured Spinal Cord.	Stem Cells	29(12) 1983-1994	2011
Nori S, Okada Y, Yasudaa A, Tsuji O, Takahashi Y, Kobayashia Y, Fujiyoshi K, Koike M, Uchiyama Y, Ikeda E, Toyama Y, Yamanaka S, Nakamura M, Okano H	Grafted human-induced pluripotent stem-cell–derived neurospheres promote motor functional recovery after spinal cord injury in mice.	PNAS	108(40) 16825-16830	2011
Yamane J, Ishibashi S, Sakaguchi M, Kuroiwa T, Kanemura Y, Nakamura M, Miyoshi H, Sawamoto K, Toyama Y, Mizusawa H, Okano H	Transplantation of human neural stem/progenitor cells overexpressing Galectin-1 improves functional recovery from focal brain ischemia in the Mongolian gerbil.	Molecular Brain	27 4:35	2011
Shang J, Deguchi K, Ohta Y, Liu N, Zhang X, Tian F, Yamashita T, Ikeda Y, Matsuura T, Funakoshi H, Nakamura T, Abe K	Strong neurogenesis, angiogenesis, synaptogenesis, and antifibrosis of hepatocyte growth factor in rats brain after transient middle cerebral artery occlusion.	J Neurosci Res	89(1) 86-95	2011
Noma S, Ohya-Shimada W, Kanai M, Ueda K, Nakamura T, Funakoshi H	Overexpression of HGF attenuates the degeneration of Purkinje cells and Bergmann glia in a knockin mouse model of spinocerebellar ataxia type 7.	Neurosci Res	in press	2012

総説

著者	論文タイトル	掲載誌名	巻 頁	出版年
青木 正志、割田 仁、糸山 泰人	ALSに対するヒト型組み換えHGF蛋白を用いた第1相試験(治験)	JALSA	82 10-12	2011
野間 さつき、船越 洋、中村 敏一	広範囲血液・尿検査、免疫学的検査(4) ーその数値をどう読むかー 肝細胞増殖因子(HGF)	日本臨床	68 増刊号7(4) 121-130	2010
船越 洋、金井 将昭、中村 敏一	トリプトファン代謝と高次脳機能	アミノ酸研究	3(1) 15-19	2010
Funakoshi H., and Nakamura T	Hepatocyte Growth Factor (HGF): Neurotrophic Functions and Therapeutic Implications for Neuronal Injury/Diseases.	Current Signal Transduction Therapy	6 156-167	2011
Funakoshi H, Kanai M, and Nakamura T	Modulation of Tryptophan Metabolism, promotion of neurogenesis and Alteration of Anxiety-Related Behavior in Tryptophan 2,3-Dioxygenase-Deficient Mice.	International Journal of Tryptophan Research	4 7–18	2011
Kadoyama K, Kadoyama K, Funakoshi H, Nakamura T, Sakaeda T	Therapeutic Potential of Hepatocyte Growth Factor for Treating Neurological Diseases.	Current Drug Therapy	6(3) 197-206	2011

Experimental Neurology 224 (2010) 403–414

Contents lists available at ScienceDirect

Experimental Neurology

journal homepage: www.elsevier.com/locate/yexnr

Anti-IL-6-receptor antibody promotes repair of spinal cord injury by inducing microglia-dominant inflammation

Masahiko Mukaino [a,b], Masaya Nakamura [c,*], Osamu Yamada [b], Seiji Okada [d], Satoru Morikawa [e], Francois Renault-Mihara [b], Akio Iwanami [c,f], Takeshi Ikegami [c,f], Yoshiyuki Ohsugi [g], Osahiko Tsuji [c], Hiroyuki Katoh [f], Yumi Matsuzaki [b], Yoshiaki Toyama [c], Meigen Liu [a], Hideyuki Okano [b,*]

[a] Department of Rehabilitation Medicine, Keio University School of Medicine, Shinjuku, Tokyo 160-8582, Japan
[b] Department of Physiology, Keio University School of Medicine, Shinjuku, Tokyo 160-8582, Japan
[c] Department of Orthopedic Surgery, Keio University School of Medicine, Shinjuku, Tokyo 160-8582, Japan
[d] Department of Research Superstar Program Stem Cell Unit, Graduate School of Medical Science, Kyushu University, Fukuoka 812-8582, Japan
[e] Department of Dentistry and Oral Surgery, Keio University School of Medicine, Shinjuku, Tokyo 160-8582, Japan
[f] National Hospital Organization, Murayama Medical Center, Musashimurayama, Tokyo 208-0011, Japan
[g] Chugai Pharmaceutical Co. Ltd., Chuo, Tokyo 103-8324, Japan

ARTICLE INFO

Article history:
Received 16 October 2009
Revised 29 April 2010
Accepted 30 April 2010
Available online 16 May 2010

Keywords:
Spinal cord injury
Interleukin-6
Antibody
Inflammation
Microglia
Hematogenous macrophages

ABSTRACT

We previously reported the beneficial effect of administering an anti-mouse IL-6 receptor antibody (MR16-1) immediately after spinal cord injury (SCI). The purpose of our present study was to clarify the mechanism underlying how MR16-1 improves motor function after SCI. Quantitative analyses of inflammatory cells using flow cytometry, and immunohistochemistry with bone marrow-chimeric mice generated by transplanting genetically marked purified hematopoietic stem cells, revealed that MR16-1 dramatically switched the central player in the post-traumatic inflammation, from hematogenous macrophages to resident microglia. This change was accompanied by alterations in the expression of relevant cytokines within the injured spinal cord; the expression of recruiting chemokines including CCL2, CCL5, and CXCL10 was decreased, while that of Granulocyte/Macrophage-Colony Stimulating Factor (GM-CSF), a known mitogen for microglia, was increased. We also showed that the resident microglia expressed higher levels of phagocytic markers than the hematogenous macrophages. Consistent with these findings, we observed significantly decreased tissue damage and reduced levels of myelin debris and Nogo-A, the axonal growth inhibitor, by MR16-1 treatment. Moreover, we observed increased axonal regeneration and/or sprouting in the MR16-1-treated mice. Our findings indicate that the functional improvement elicited by MR16-1 involves microglial functions, and provide new insights into the role of IL-6 signaling in the pathology of SCI.

Introduction

In the pathology of spinal cord injury (SCI), the primary mechanical injury is followed by post-traumatic inflammation, in which inflammatory cells such as neutrophils, hematogenous macrophages (blood-borne macrophages), and resident microglia accumulate at the lesion site. These inflammatory cells release reactive oxygen, nitrogen radicals, and proteases, which exacerbate tissue damage (Hausmann, 2003). Because the inflammation is regulated by pro-inflammatory cytokines, such as TNFα, IL-1β, and IL-6, these cytokines have been targets for potential pharmaceutical interventions for SCI (Nesic et al., 2001; Okada et al., 2004; Sharma et al., 2003; Tuna et al., 2001). Among these cytokines, IL-6 is known to promote the activation and infiltration of macrophages/microglia (Hurst et al., 2001; Van Wagoner and Benveniste, 1999), which are the major inflammatory cells in the injured spinal cord, and the overexpression of IL-6 extends the inflammation to worsen the tissue injury (Klusman and Schwab, 1997; Lacroix et al., 2002). Hypothesizing that a blockade of IL-6 signaling might reduce the extension of injury by post-SCI inflammation, we previously administered the anti-mouse IL6-receptor antibody (MR16-1) after SCI and demonstrated reduced inflammation, decreased astrogliosis, and enhanced tissue sparing, leading to improved functional recovery (Okada et al., 2004). As a humanized antibody for the human IL-6 receptor (MRA; tocilizumab) is already in clinical use for the treatment of Castleman's disease and rheumatoid arthritis (Choy et al., 2002; Nishimoto et al., 2000; Sato et al., 1993), this drug might represent a new option for the treatment of SCI.

* Corresponding authors. H. Okano is to be contacted at the Department of Physiology, Keio University School of Medicine, 35 Shinanomachi, Shinjuku, Tokyo 160-8582, Japan. M. Nakamura, Department of Orthopedic Surgery, Keio University School of Medicine, Shinjuku, Tokyo 160-8582, Japan. Fax: +81 3 3357 5445.
E-mail addresses: masa@sc.itc.keio.ac.jp (M. Nakamura), hidokano@sc.itc.keio.ac.jp (H. Okano).

0014-4886/$ – see front matter © 2010 Elsevier Inc. All rights reserved.
doi:10.1016/j.expneurol.2010.04.020

However, recent studies using gene-knockout animals revealed that the continuous inhibition of IL-6 signaling is detrimental to functional recovery, by inhibiting axonal regeneration or causing failed gliosis, implying that IL-6 may also have a beneficial function in spinal cord repair (Cafferty et al., 2004; Okada et al., 2006). Furthermore, numerous studies suggest that inflammation is beneficial or even essential for spinal cord repair, because it clears tissue debris and involves the secretion of various neurotrophic factors (Donnelly and Popovich, 2008; Hashimoto et al., 2005; McTigue et al., 2000). This discrepancy prompted us to investigate how the administration of an anti-IL-6 receptor antibody immediately after SCI promotes the repair process.

One of the important determinants of the extent of secondary damage by inflammation is the nature of the recruited inflammatory cells. For example, the transplantation of macrophages that have been co-incubated with peripheral nerves or skin improves spinal cord repair (Bomstein et al., 2003; Schwartz et al., 1999). On the other hand, zymosan-activated macrophages have neurotoxic properties, although they can also have proregenerative effects (Gensel et al., 2009; Popovich et al., 2002; Steinmetz et al., 2005). Previous reports have shown that these differences in the characteristics of inflammatory cells depend not only on their state of activation, but also on their origin. A subpopulation of hematogenous macrophages is more cytotoxic than microglia, and their excessive infiltration into a lesion is detrimental to spinal cord repair (Gris et al., 2004; Popovich et al., 1999). Since IL-6 is known to promote macrophage infiltration after central nervous system (CNS) trauma (Klusman and Schwab, 1997; Lacroix et al., 2002), here we focused on the effect of the temporary inhibition of IL-6 signaling by MR16-1 on macrophages and microglia after SCI. The administration of MR16-1 reduced the infiltration of macrophages into the injured spinal cord, but increased the number of microglia residing there, thus switching the major inflammatory cell type at the lesion from hematogenous macrophages to resident microglia. A comparison of the expression of phagocytic markers by hematogenous macrophages and microglia revealed that the microglia had greater phagocytic ability against myelin debris after SCI. Consequently, this switch in major inflammatory cell type resulted in improved tissue sparing and debris clearance, which promoted neural repair after SCI.

Materials and methods

Animals

74 adult female C57BL/6J mice (8–10 weeks old) were used. C57BL/6 background CAG-EGFP transgenic mice that ubiquitously express EGFP under the control of the CAG promoter (Kawamoto et al., 2000) were kindly provided by Professor Jun-ichi Miyazaki (Osaka University, Osaka, Japan) and were bred in our animal facility. The ethics committee of our institution approved all the surgical and animal care procedures, in accordance with the Laboratory Animal Welfare Act, the Guide for the Care and Use of Laboratory Animals (National Institutes of Health), and the Guidelines and Policies for Animal Surgery provided by the Animal Study Committees of the Central Institute for Experimental Animals and of Keio University.

Rat anti-mouse IL-6 receptor monoclonal antibody (MR16-1)

The rat anti-mouse IL-6 receptor monoclonal antibody MR16-1 was prepared as described previously (Tamura et al., 1993). MR16-1 binds to the mouse IL-6 receptor and suppresses IL-6-induced cellular responses in a dose-dependent manner (Okazaki et al., 2002). Other basic characterizations of this antibody were reported previously (Okazaki et al., 2002; Tamura et al., 1993).

Purification and transplantation of genetically marked hematopoietic stem cells (HSCs)

In the present study, we produced bone marrow-chimeric mice using highly purified, genetically marked hematopoietic stem cells by the method reported by Koide et al. (2007). This method enabled us to limit our observation specifically to the hematopoietic cell lineage. The femurs and tibias were dissected from donor CAG-EGFP transgenic mice and crushed with a pestle. The marrow cells were collected in HBSS+ (Hanks-balanced salt solution supplemented with 2% FCS, 10 mM HEPES, and 1% penicillin/streptomycin), filtered through a cell strainer (Falcon 2350) to remove debris, and suspended in 50 ml of ice-cold HBSS+. The cells were collected by centrifugation at 280 *g* for 6 min at 4 °C, resuspended in HBSS+ at 1×10^6 cells/ml, and incubated with 5 μg/ml Hoechst 33342 (Sigma Chemical Co.) for 60 min at 37 °C. A parallel aliquot was stained with Hoechst dye in the presence of 50 μM reserpine (Sigma Chemical Co.). The cells were spun down, resuspended in 5 ml of ice-cold HBSS+, and layered on top of 5 ml of Ficoll-Paque™ Plus (Amersham Pharmacia Biotech AB, Uppsala, Sweden). After centrifugation at 630 *g* at 4 °C for 20 min, the mononuclear cells were collected from the intermediate layer and immediately washed with 10 ml of ice-cold HBSS+. The Hoechst-stained cells were resuspended in ice-cold HBSS+ at $1–5\times10^7$ cells/ml and stained for 30 min on ice with one of the following monoclonal antibodies: biotinylated CD34 (RAM34), PE-conjugated Sca-1 (Ly6A/E), or APC-conjugated c-Kit (2B8). Biotinylated antibodies were visualized with Cy7-APC-conjugated streptavidin. All of these reagents were purchased from eBioscience (San Diego, CA). An aliquot of cells was also stained with a mouse isotype control conjugated with FITC, PE, or APC. After antibody staining, the cells were washed in an excess volume of HBSS+ and resuspended at 1×10^7 cells/ml in HBSS+ containing 2 μg/ml propidium iodide (PI; Sigma Chemical Co.). Genetically marked, highly purified HSCs ($CD34^-$ $Sca\text{-}1^+$ $c\text{-}kit^+$ SP cells (Matsuzaki et al., 2004)) derived from donor CAG-EGFP transgenic animals were sorted by flow cytometry. A 100-μl aliquot of unfractionated marrow cell suspension (2×10^5 cells) from donors not carrying the CAG-EGFP transgene was added to provide competitor cells, which is the minimum dose to keep the animals alive during the period required for bone marrow reconstitution. A suspension of 100 $CD34^-$ $Csa\text{-}1^+$ $c\text{-}kit^+$ SP cells and 2×10^5 unfractionated marrow cells was then intravenously injected into the retro-orbital plexus of an etherized recipient mouse that had been lethally irradiated at 10.5 Gy. The successful induction of chimerism was confirmed by a Dual-laser FACS Calibur (Becton and Dickinson, CA) analysis of the peripheral blood.

Spinal cord injury model

Mice were anesthetized with an intraperitoneal injection of ketamine (100 mg/kg) and xylazine (10 mg/kg). The dorsal surface of the dura mater at the T10 level was exposed by laminectomy, and a moderate (impact force = 60 kdyn) contusion injury was induced using an IH impactor, as reported previously (Cafferty et al., 2004; Glass et al., 2001). The muscles and skin were closed in layers, and the animals were placed in a temperature-controlled chamber until thermoregulation was reestablished. Manual voiding of the bladder was performed twice per day until reflex bladder emptying was reestablished.

Injection of MR16-1 and BrdU

Immediately after SCI, mice were given a single intraperitoneal injection of MR 16-1 (100 μg/g body weight; MR16-1-treated group) or the same volume and concentration of purified rat IgG (ICN/Cappel Ohio; control group). To label the cells that divided after the injury, a sterile solution of bromodeoxyuridine (BrdU; 50 μg/g body weight; Sigma) was injected intraperitoneally immediately after the injury, and then every 24 h for 4 days after SCI (a total of 5 times).

Immunohistochemistry

At 4, 7, 14, and 42 days after SCI, animals in the MR16-1-treated and control groups were deeply anesthetized by inhalation of diethyl ether and transcardially perfused with 4% paraformaldehyde in 0.1 M phosphate-buffered saline (PBS). The spinal cord tissue was removed and post-fixed in 4% paraformaldehyde in PBS for a few hours at room temperature. The tissue samples were immersed in 10% sucrose in PBS at 4 °C for 24 h, then placed in 30% sucrose in PBS for 48 h, and embedded in OTC compound. The embedded tissue was immediately frozen in liquid nitrogen and stored at −80 °C until use. Frozen spinal cord tissues were sectioned on a cryostat at 20 μm, either in the axial or sagittal plane. Luxol fast blue and Oil red O staining were performed to evaluate the spared myelin and myelin debris.

For immunohistochemistry with fluorescent antibodies, spinal cord sections were permeabilized with 0.03% Triton X-100 and 10% normal goat serum in 0.01 M PBS, pH 7.4, for 30 min. The following primary antibodies were applied overnight at 4 °C: rat anti-CD11b, 1:200 (Serotec, Oxford, United Kingdom); rabbit anti-Iba-1, 1:200 (Wako Pure Chemical Industries, Osaka, Japan); rat anti-LAMP2, 1:200 (Abcam, Cambridge, UK); rat anti-Mac2, 1:200 (Cedarlane, Hornby, Ontario); rabbit anti-GFP, 1:500 (MBL, Nagoya, Japan); goat anti-GFP, 1:500 (Rockland Immunochemicals, Gilbertsville, PA); or chick anti-GFP, 1:500 (Aves Lab, Tigard, OR). The sections were then incubated for 1 h at room temperature with secondary antibodies conjugated with Texas red or fluorescein isothiocyanate (FITC; all from Jackson Immunoresearch, West Grove, PA). The sections were then washed, wet-mounted, and examined by epi-fluorescence. Multiple staining with Oil red O was performed by the method reported by Koopman et al. (2001).

For diaminobenzidine (DAB; Sigma) staining, mouse anti-Neurofilament 200kD antibody, 1:200 (Chemicon, Temecula, CA) or goat anti-5HT, 1:200 (Immunostar, Hudson, WI) was used as the primary antibody, followed by horseradish peroxidase (HRP)-labeled goat anti-mouse IgG or donkey anti-goat IgG as the secondary antibody. The staining was visualized with DAB, and the sections were washed, dehydrated, cleared in xylene, and mounted.

Quantitative analyses

For quantitative analyses, three representative midsagittal or axial sections through the injured portion of the spinal cord of each mouse were selected randomly and captured at 50× magnification. The areas of tissue immunopositive for CD11b, Iba-1, LAMP2, Mac2, Neurofilament 200kD, and Nogo-A, and those stained with Oil red O (ORO) and Luxol Fast Blue (LFB) were quantified using the ImageJ software and MCID system (Imaging Research, Inc., St. Catharines, Ontario, Canada). To count the number of macrophages/microglia, three midsagittal sections through the injured portion of the spinal cord of each mouse were selected randomly, and the number of CD11b- or Iba-1- and/or EGFP-immunopositive cells contained within a cephalocaudal stretch of 500 μm at the indicated levels was counted. To confirm the CD11b-Iba-1 double-staining as a marker of macrophages/microglia the ratio of CD11b-Iba-1 double-stained cells to total CD11b-positive cells was also quantified. To count the LAMP2- andMac2-positive cells, three midsagittal sections through the injured portion of the spinal cord of each mouse were selected randomly, and a threshold was determined from the basal fluorescence of a portion of intact tissue. From the epicenter area (0–1-mm caudal and rostral to the epicenter), 15 non-overlapping high-power fields were chosen at random (630× magnification; total area 0.39 mm^2). An immunopositive cell was defined as a cell with staining over 10% of its soma, as determined by the MCID system, and the number of stained and unstained cells was counted manually. For the quantification of $5HT^+$ fibers, five regions (the dorsal horn and ventral horn of both sides, and the site around the central canal) from each axial section of the cord, 2-mm caudal to the epicenter, were captured at ×200 magnification, and the area of the $5HT^+$ tissue in each field was quantified using the MCID system. The light intensity and threshold values were maintained at constant levels for all analyses.

Flow cytometry

Mice were transcardially perfused with 0.1 M phosphate-buffered saline, and the spinal cords were harvested. The injured portion of each spinal cord (6 mm) was surgically dissected, digested with collagenase, mechanically homogenized, and passed through a wire mesh screen (Sigma-Aldrich Canada Ltd., Ontario, Canada) to obtain a single-cell suspension. The cells were washed in PBS containing 3% FBS, and incubated for 5 min on ice with Fc Block and 30 min on ice with fluorescent antibodies. Flow cytometric analysis was performed using a FACS Calibur (Becton Dickinson) and MoFlo (Dakocytomation), and the data were analyzed using Cell Quest software. The cells were stained with antibodies against CD11b-PE, CD45-FITC, and CD45-APC (eBioscience, San Diego, CA), and were classified according to their expression level of CD45 (common leukocyte antigen) and CD11b (complement 3 receptor), with $CD11b^+$ $CD45^{high}$ indicating hematogenous macrophages and $CD11b^+$ $CD45^{low}$ indicating resident microglia, as reported previously (Sedgwick et al., 1991). At least 1.0×10^6 cells were analyzed for each spinal cord sample.

Western blot analysis

Twenty-four hours after the injury, the spinal cord tissue at the lesion epicenter (6 mm in length) was dissected from the mice (four animals per group and four sham-operated animals), homogenized in MAPK lysis buffer containing protease inhibitors, sonicated, and spun at 15,000 rpm. The proteins in the supernatants were separated by 10% SDS-PAGE and transferred to a polyvinylidene difluoride membrane by electrophoresis. The membranes were blocked for 1 h at room temperature in TBST buffer containing 4% non-fat milk, NaCl (150 mM), and 0.05% Tween 20. The blots were then incubated with primary polyclonal rabbit anti-CCL2 antibody (1:2000; Abcam, Cambridge, MA), goat anti-CCL5 antibody, 1:500 (eBioscience, San Diego, CA); rabbit anti-CXCL-10 antibody, 1:500 (Cedarlane, Hornby, Ontario); rabbit anti-GM-CSF antibody, 1:2000 (Abcam, Cambridge, MA); or mouse anti-α-tubulin antibody, 1:500 followed by a secondary HRP-conjugated anti-rabbit, goat, or mouse IgG antibody. The blots were visualized with the ECL Blotting Analysis System (Amersham, Arlington Heights, IL).

Real time RT-PCR

A 4-mm-long spinal cord segment at T10 was collected at the indicated times, the total RNA was isolated using an RNeasy Kit (Qiagen Science, Maryland, USA), and cDNA was obtained by reverse transcription. The cDNA synthesis was performed at 42 °C for 50 min in a final volume of 20 μl, following the manufacturer's instructions for Superscript II RNase H Reverse Transcriptase (Invitrogen). The template cDNA was normalized to the β-actin mRNA. Real time RT-PCR was performed using an Mx3000P thermal cycler (Stratagene) with SYBR green (TaKaRa RR041A). For every set of RT-PCR analyses, at least three independent experiments were performed. The amplification was performed using the following primers: CCL2, sense 5′-GCATCCACGTGTTGGCTCA-3′, antisense 5′-CTCCAGCCTACT-CATTGGGATCA-3′; CCL5, sense 5′-AGATCTCTGCAGCTGCCCTCA-3′, antisense 5′-GGAGCACTTGCTGCTGGTGTAG-3′; CXCL10, sense 5′-TGAATCCGGA ATCTAAGACCATCAA-3′, antisense 5′-AGGACTAGC-CATCCACTGG GTAAAG-3′ (purchased from Takara, Kyoto, Japan) and GM-CSF, sense 5′-AAGGTCCTGAGGAGGA TGTG-3′, antisense 5′-GAGGTTCAGGGCTTCTTTGA-3′ (purchased from Hokkaido System Science, Sapporo, Japan).

Statistical analysis

Values are reported as the mean ± SEM. Statistical significance was analyzed using the unpaired Student's *t*-test, and significance was accepted at $P<0.05$.

Results

Anti-IL-6 receptor antibody treatment reduced inflammatory cell accumulation

To examine the effect of MR16-1 on the infiltration of inflammatory cells after SCI, immunostaining for CD11b and Iba-1 was performed. Although CD11b is known to be expressed by granulocytes and some T cells, 93.6 ± 3.3% of the infiltrated cells were CD11b and Iba-1 double-positive at 4, 7, and 14 days post-injury (dpi), indicating that the immunocompetent cells present at the injured site at those times after SCI were mostly hematogenous macrophages and resident microglia (Figs. 1A–E). While the CD11b-positive area increased in both the MR16-1 and control groups, with a peak at 7 dpi, the MR16-1-treated animals showed a significantly smaller $CD11b^+$ area compared to the control animals: a non-significant difference at 4 and 7 dpi that developed to a significant difference at 14 dpi (Fig. 1F). These findings suggest that MR16-1 administration reduced the accumulation of $CD11b^+$ cells at the late stage of inflammation, even though MR16-1 was only administered once, at the acute stage.

To determine whether the administration of MR16-1 alters the subtype of $CD11b^+$ cells at the acute stage, the profiles of the recruited $CD11b^+$ cells were analyzed using flow cytometry. Homogenates of the injured spinal cord were analyzed to determine the ratio of hematogenous macrophages to total $CD11b^+$ cells. We first confirmed that within the $CD11b^+$ population, hematogenous macrophages could be distinguished from the resident microglia by their expression level of CD45, as reported previously (Sedgwick et al., 1991). At 4 dpi, 37.6 ± 3.9% of the $CD11b^+$ cells were $CD45^{high}$ hematogenous macrophages in the control group, whereas only 22.3 ± 2.9% of these cells were $CD45^{high}$ in the MR16-1-treated group. Although the proportion of hematogenous macrophages had increased in both groups at 7 dpi, the difference in their proportions between the MR16-1-treated and control mice was significant (57.8 ± 1.9% in the control group, 41.0 ± 2.2% in the MR16-1-treated group) (Figs. 1G–I). MR16-1 treatment thus reduced the relative abundance of hematogenous macrophages in the injured spinal cord.

MR16-1 treatment caused the central player in the inflammation after SCI to shift from hematogenous macrophages to resident microglia

To determine whether MR16-1 specifically affects the recruitment of hematogenous macrophages into the injured spinal cord, contusive SCI was induced in chimeric mice, which were generated by irradiating

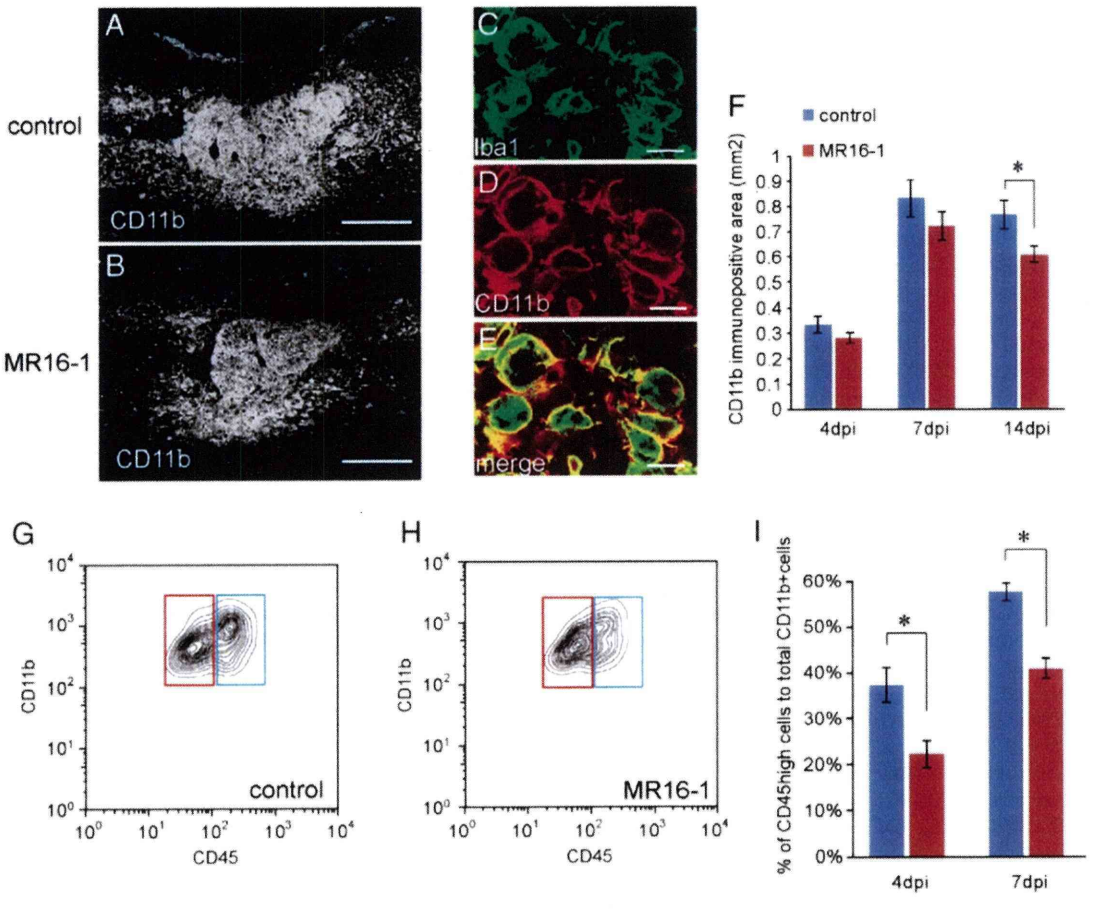

Fig. 1. MR16-1 treatment accelerates the resolution of inflammation. A, B, F: There was a significant difference in the $CD11b^+$ area between the control group (A) and the MR16-1-treated group (B) at 14 dpi, but not at 4 or 7 dpi (F). C–E: 96.9 ± 1.3% of the $CD11b^+$ cells (D) were double-labeled with Iba1 (C, E), indicating that the accumulated $CD11b^+$ cells were inflammatory macrophages/microglia. G–I: MR16-1-treatment decreased the proportion of hematogenous macrophages in the injured spinal cord at 4 and 7 dpi. Hematogenous macrophages ($CD11b^+CD45^{high}$, blue box) and microglia ($CD11b^+CD45^{low}$, red box) were identified according to their levels of CD11b and CD45 expression. I: The proportion of hematogenous macrophages within the $CD11b^+$ population was significantly lower in the MR16-1-treated animals than in the control group at 4 and 7 dpi. Values are means ± SEM. *$P<0.05$. Scale bars = 500 μm in A, B; 20 μm in C–E.

recipient mice and then transplanting purified EGFP-expressing HSCs into them (Matsuzaki et al., 2004). Flow cytometric analysis revealed that 3 months after the HSC transplantation, 88.34±1.45% of the CD11b$^+$ leukocytes in the blood of the chimeric mice were EGFP-positive. In contrast, only 1.57% of the CD11b$^+$ cells in the uninjured spinal cord expressed EGFP, suggesting that the recruitment of microglia from the hematopoietic pool was a rare event. Since the irradiation dose required for this method is rather high (10.5 Gy), which could affect microglial turnover (Mildenberger et al., 1990), we quantified the accumulation of CD11b+ cells at the lesion of chimeric mice, and compared it to that of wild-type mice. There was no significant difference in the number of CD11b+ cells between the chimeric mice and wild-type mice at 4, 7, or 14 dpi (P=0.60, 0.76, 0.67, respectively). This result is consistent with the previous report by Turrin et al. (2007), which showed that the chimerization with 10 Gy irradiation dose does not significantly affect the acute inflammatory response. Thus, these chimeric mice enabled us to distinguish in situ hematogenous macrophages from endogenous microglia by their EGFP immunoreactivity (Figs. 2A–C), and examine the precise spatio-temporal localization of these cell populations after SCI.

Consistent with our findings using wild-type mice, the total number of recruited CD11b$^+$ macrophages/microglia was comparable between the MR16-1-treated and control groups at 4 dpi (not shown), but the proportion and distribution of the hematogenous macrophages and microglia were completely different (Figs. 2D, E, G, and I). In the MR16-1-treated group, there were significantly fewer CD11b$^+$EGFP$^+$ hematogenous macrophages at the lesion site (Fig. 2G), and there were significantly more CD11b$^+$EGFP$^-$ resident microglia, especially in areas 1.0- to 2.0-mm away from the lesion site (Fig. 2I). Thus, at 4 dpi, the MR16-1 treatment led to a reduced accumulation of hematogenous macrophages at the lesion epicenter, and an increased number of microglia at sites rostral and caudal to the lesion epicenter.

Similarly, at 7 dpi, although the distribution of CD11b$^+$ cells was comparable in the control and MR16-1-treated groups (Fig. 2F), the composition of the CD11b$^+$ population was dramatically different. In the MR16-1-treated group, the CD11b$^+$EGFP$^+$ hematogenous macrophage accumulation at the lesion epicenter was significantly reduced (Fig. 2H), and the CD11b$^+$EGFP$^-$ resident microglia had significantly increased (Fig. 2J). These results indicate that the central player in the inflammation after SCI shifted from being hematogenous macrophages to being resident microglia, following MR16-1-treatment.

MR16-1 treatment reduced the expression of macrophage-recruiting chemokines and increased the GM-CSF level at the lesion site

Although there is no evidence that IL-6 directly stimulates the infiltration or proliferation of inflammatory cells, it does affect the expression of various cytokines; furthermore, the blockade of IL-6 signaling during inflammation causes a drastic change in the cytokine profile, including the chemokines and colony-stimulating factors (CSFs) (Matsumura et al., 1999; Romano et al., 1997). Because the infiltration of hematogenous macrophages is mediated by chemokines (Babcock et al., 2003; Romano et al., 1997) and the increased proliferation of microglia is mainly controlled by CSFs (Giulian and Ingeman, 1988; Lee et al., 1994), we examined the expression levels of CCL2 (MCP-1), CCL5 (RANTES), CXCL10 (IP-10), and GM-CSF, which are representative cytokines known to direct cell infiltration and proliferation, by quantitative real time PCR, 12 h after injury. The mRNA levels of CCL2, CCL5, and CXCL10 were significantly attenuated by MR16-1-administration compared to the control group (to 15.0%, 49.7% and 30.8% of the control levels, respectively), whereas the GM-CSF mRNA level was significantly increased (to 214% of the control level) (Figs. 3A–D). We also quantified the cytokine proteins by western blotting. The protein level of CCL2 was significantly decreased (to 80.7% of the control level), whereas the GM-CSF level was significantly increased (to 193% of the control level). Although the difference did not reach to statistical significance, we also observed a tendency for the protein levels of CCL5 and CXCL10 to decrease (Figs. 3E–H).

Microglia had higher phagocytic capacities than hematogenous macrophages

To determine whether the shift in the major inflammatory cells by MR16-1 treatment affected the inflammatory process, we further characterized the hematogenous macrophages and the microglia. The phagocytosis of tissue debris by inflammatory cells is a pivotal process for spinal cord repair after injury, as the debris includes various cytotoxic agents and axonal growth inhibitory factors. Quantitative analysis revealed that the expression of LAMP2, a marker for endosomes/lysosomes, was significantly increased at the lesion epicenter in the MR16-1-treated group compared to the control group, at 4, 7, and 14 dpi (Figs. 4A–C). Previous reports showed that the resident microglia have higher phagocytic activity than the infiltrating hematogenous macrophages (Rinner et al., 1995; Schilling et al., 2005). Consistent with these reports, we found that significantly more Iba1$^+$EGFP$^-$ resident microglia expressed LAMP2 than did the Iba1$^+$EGFP$^+$ hematogenous macrophages at 4 and 7 dpi (Figs. 4D–G).

In addition, we performed immunostaining with Mac2, which is reported to participate in the phagocytosis of myelin (Rotshenker et al., 2008). Although Mac2 was expressed on the cell membrane of most of the accumulated cells, only a portion of the macrophages/microglia expressed Mac2 in their cytoplasm. Consistent with the LAMP2 results, more of the Iba1$^+$EGFP$^-$ resident microglia than Iba1$^+$EGFP$^+$ hematogenous macrophages showed cytoplasmic expression of Mac2 (Figs. 5A–D, and I). Similarly, the average size and intracellular Mac2$^+$ area of the resident microglia were significantly greater at 7 dpi than those of hematogenous macrophages (Figs. 5J and K). We also performed triple staining for Iba-1, EGFP, and Oil red O using the method reported by Koopman et al. (2001) to observe phagocytosed lipid, which is derived from myelin. The Oil red O$^+$ area in each cell body was significantly greater in the Iba1$^+$EGFP$^-$ resident microglia than in the Iba1$^+$EGFP$^+$ hematogenous macrophages, and was increased at 7 dpi by the MR16-1 treatment (Figs. 5E–H, L).

MR16-1 treatment promotes repair of the spinal cord

To examine the effect of the altered inflammatory response on spinal cord repair, we evaluated the clearance of myelin debris by Oil red O staining and Nogo-A immunostaining, as well as the sparing of myelin sheath, which is evaluated by Luxol Fast Blue staining. At 14 and 42 dpi, the Oil red O$^+$ area was significantly decreased in the MR16-1-treated group compared to the control group (Figs. 6A–C). The deposition of Nogo-A, the major myelin-derived axonal growth inhibitor, was also decreased by MR16-1 treatment (Figs. 6D–F). Furthermore, we evaluated the spared myelin sheath using Luxol fast blue staining. At the lesion epicenter, the area of the spared myelin sheath in the MR16-1-treated group was significantly greater than in the control group at 14 and 42 dpi (Figs. 6G–I).

To determine the effect of MR16-1 on repair of neural tissue, we quantified the RT-97$^+$ (Neurofilament 200kD) fibers at the lesion epicenter and the 5-HT$^+$ (serotonergic) fibers that were caudal to the lesion site. There was no significant difference in the area of RT-97$^+$ fibers between the two groups at 14 dpi, but a significantly larger RT-97$^+$ area was observed in the MR16-1-treated group at 42 dpi (Figs. 6J–K). Similarly, there was no significant difference in the 5-HT$^+$ area between the two groups at 14 dpi. Although there was a slight increase in 5-HT$^+$ fibers at 42 dpi, even in the control group, which is characteristic of contusive SCI, a significantly larger area of 5-HT$^+$

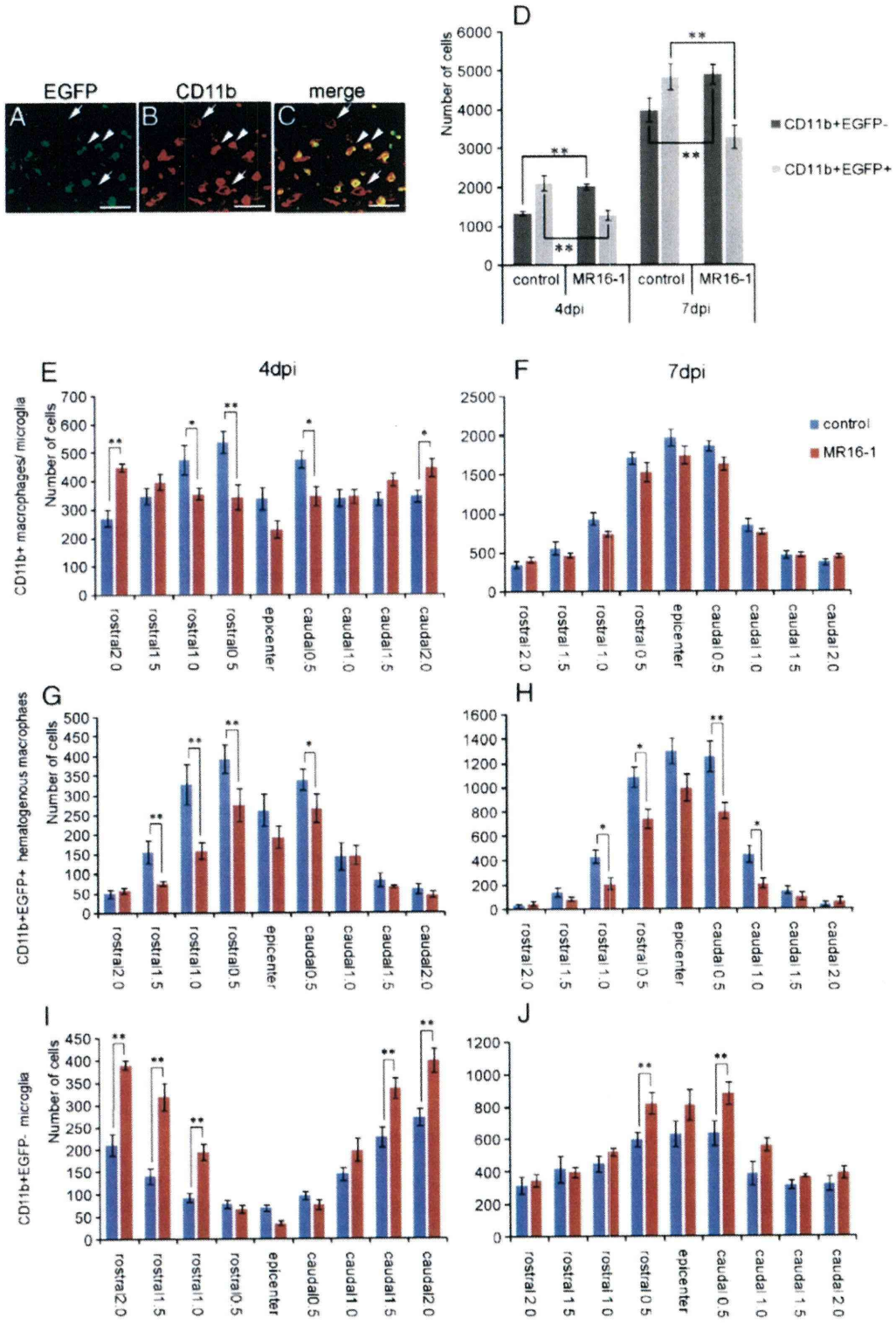

Fig. 2. MR16-1 treatment switches the major inflammatory cell type, from hematogenous macrophages to resident microglia. Analysis using chimeric mice. A–C: Immunostaining for EGFP (A, green) and CD11b (B, red), showing the distribution of $CD11b^+EGFP^+$ hematogenous macrophages (arrowheads) and $CD11b^+$ $EGFP^-$ resident microglia (arrows) in the injured spinal cord (C, merged). D: In the MR16-1-treated group, the major player in the inflammation switched from $CD11b^+EGFP^+$ hematogenous macrophages (light gray) to $CD11b^+EGFP^-$ resident microglia (dark gray) at 4 and 7 dpi. Number and distribution of macrophages/microglia in the spinal cord at 4 and 7 dpi. E, F: MR16-1 did not significantly affect the total number of inflammatory cells ($Cd11b^+$) at 4 (E) or 7 (F) dpi. G, H: MR16-1 reduced the recruitment of $CD11b^+EGFP^+$ hematogenous macrophages at 4 (G) and 7 (H) dpi. I, J: MR16-1 treatment increased the number of $CD11b^+EGFP^-$ resident microglia 1.0 to 2.0 mm rostral and caudal to the lesion epicenter at 4 dpi (I). At 7 dpi, both groups showed a shift in $CD11b^+EGFP^-$ microglia to the lesion epicenter, where the number of $CD11b^+EGFP^-$ microglia was significantly higher in the MR16-1-treated animals (J). Values are means ± SEM. $^*P<0.05$. $^{**}P<0.01$. Scale bars = 50 μm in A–C.

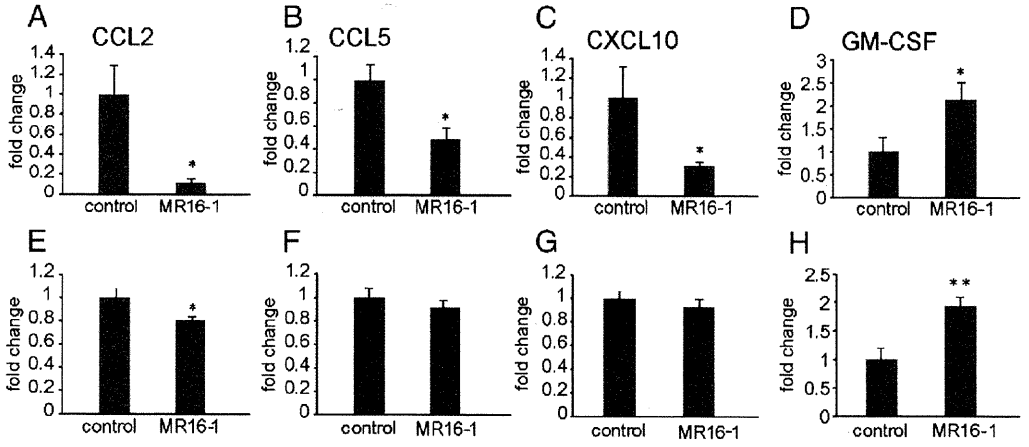

Fig. 3. MR16-1 decreases the expression level of macrophage-recruiting chemokines, while increasing that of GM-CSF. A–D: The CCL2 (A), CCL5 (B), CXCL10 (C), and GM-CSF (D) mRNA expression levels in the spinal cord tissue 12 h after injury were determined using quantitative RT-PCR. Macrophage-recruiting chemokines had significantly decreased, while the expression of GM-CSF, a known mitogen for microglia, had increased. E–H: The protein levels of the CCL2(E), CCL5(F), CXCL10(G) and GM-CSF(H) 24 h after injury were determined by western blot analysis. The protein level of CCL2 (E) was significantly decreased, whereas the GM-CSF (H) level was significantly increased. There was a tendency for the protein levels of CCL5 (F) and CXCL10 (G) to decrease, although the change was not statistically significant. Values are means ± SEM. $^{*}P<0.05$.

fibers was observed in the MR16-1-treated group than in the control group (Figs. 6M–O).

Discussion

IL-6 is a pro-inflammatory cytokine that triggers secondary injury in the pathophysiology of SCI. IL-6 binds to soluble and membrane-bound IL-6-receptor to form a complexed ligand for gp130, the common signal transducer of IL-6 and its related cytokines. MR16-1 is a neutralizing antibody for IL-6-receptor that competitively inhibits its binding to IL-6, thereby blocking IL-6-receptor-mediated cell signaling. We previously reported that the systemic administration of MR16-1 decreases the phosphorylation of signal transducer and activator of transcription 3 (STAT3) in the injured spinal cord, demonstrating that this treatment potently affects the IL-6/JAK/STAT3 signaling pathway. Subsequently, we showed that MR16-1 administration after SCI reduces the number of inflammatory cells present 2 weeks after injury and decreases the amount of reactive astrogliosis, leading to improved functional recovery (Okada et al., 2004). Our present study extends these findings, showing that MR16-1 treatment alters the nature of the inflammatory response after SCI.

Here we found that the temporary inhibition of IL-6 signaling by MR16-1 treatment caused a significant reduction in the macrophage/microglia accumulation at 14 dpi, but not at 4 or 7 dpi. We had expected MR16-1 to have an anti-inflammatory effect, because IL-6 is a pro-inflammatory cytokine, so it was unclear why the immediate administration of MR16-1 affected only the late phase of the inflammatory response after SCI. We hypothesize that the response was delayed because the effects of MR16-1 treatment were owed to changes in the nature of the inflammatory response, rather than to the immediate effects of inhibiting the IL-6 signal.

Previous studies showed that functional recovery after SCI is affected by the properties of the inflammatory response, which are determined by the cell types involved and their state of activation (Gris et al., 2004; Popovich et al., 1999; Rapalino et al., 1998; Saville et al., 2004; Schwartz et al., 1999). Hematogenous macrophages and microglia are the major players in the inflammatory pathology of SCI, and their characteristics have therefore been of major interest. Of the two, hematogenous macrophages are regarded as more detrimental, because removing them or preventing their infiltration into the injured tissue reduces the degree of secondary injury and improves functional recovery (Gris et al., 2004; Popovich et al., 1999). In contrast, microglia are believed to be relatively beneficial for spinal cord repair, owing to their higher phagocytotic activity and expression of various neurotrophic factors (Lalancette-Hebert et al., 2007; Schilling et al., 2005). The state of cell activation also affects the nature of the inflammation; the implantation of bone marrow-derived macrophages previously stimulated by co-incubation with peripheral nerve or skin improves spinal cord repair (Bomstein et al., 2003; Rapalino et al., 1998).

Because IL-6 has a leading role in recruiting macrophages during inflammation, we hypothesized that MR16-1 treatment would decrease the infiltration of hematogenous macrophages. Therefore, we focused on the balance between the types of inflammatory cells, i.e., the hematogenous macrophages and microglia. Flow cytometric analysis revealed that the proportion of infiltrated $CD45^{high}$ hematogenous macrophages decreased markedly following MR16-1 treatment, with the result that resident microglia replaced hematogenous macrophages as the major inflammatory cell type at the lesion site. Furthermore, we performed quantitative analyses in chimeric mice bearing transplanted EGFP-expressing, highly purified HSCs. These analyses showed that, besides the reduced infiltration of hematogenous macrophages following MR16-1 treatment, the number of resident microglia increased, contributing to the shift in the major inflammatory cell type. The increase in the number of BrdU+ microglia by MR16-1 indicated that the higher number of microglia might have resulted from their increased proliferation (Suppl. Fig. 1).

Two mechanisms appear to mediate this phenomenon. First, the number of hematogenous macrophages is reduced because fewer are recruited from the blood pool. Various chemokines are known to mediate macrophage infiltration; in particular, CCL2, CCL5, and CXCL10 have a demonstrated role in recruiting macrophages following CNS injury (Babcock et al., 2003; Ghirnikar et al., 1998; Glass et al., 2001; Liu et al., 2001). Here we observed decreased expression levels of CCL2, CCL5, and CXCL10 following MR16-1-treatment, which could account for the reduced infiltration of hematogenous macrophages. This agrees with the observation that IL-6 is a major player in directing chemokine-mediated macrophage infiltration during inflammation (Hurst et al., 2001; Romano et al., 1997).

In contrast to hematogenous macrophage recruitment, microglial proliferation is mainly regulated by colony-stimulating factors (CSFs) (Giulian and Ingeman, 1988; Lee et al., 1994), and the local increase in GM-CSF that we observed could have stimulated their proliferation, resulting in their increased numbers at the lesion site (Lee et al., 1994). Since IL-6, like other cytokines, interacts with various other

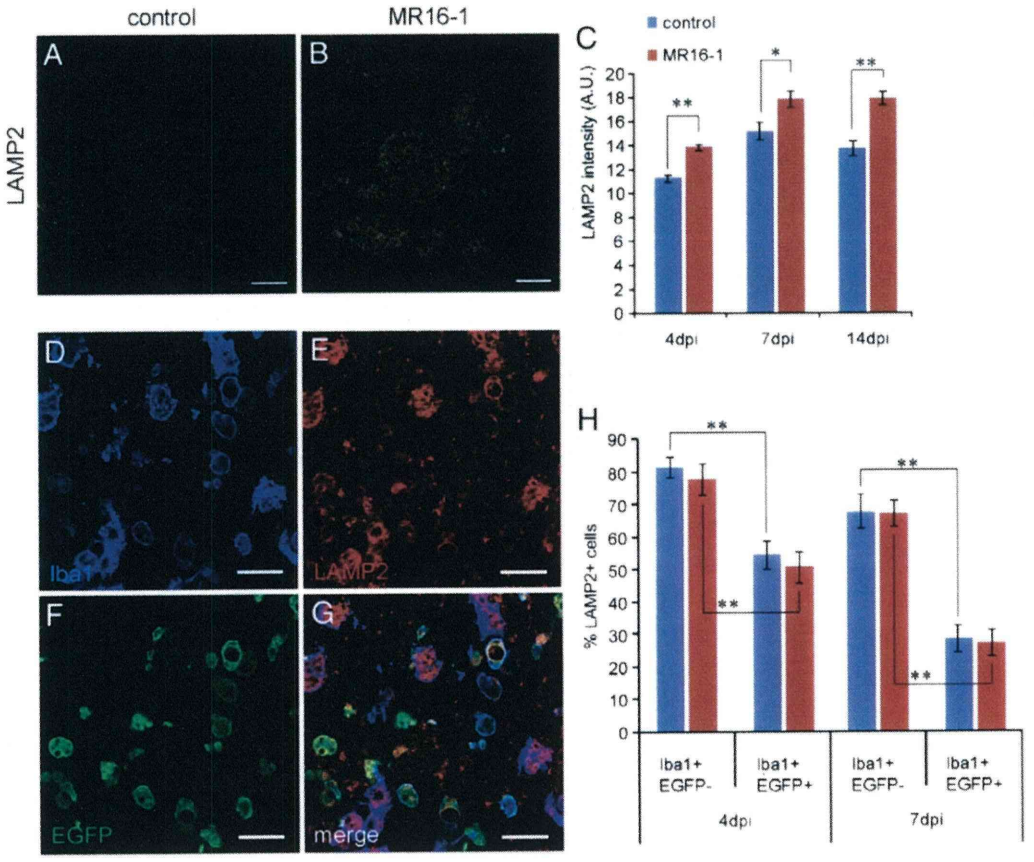

Fig. 4. MR16-1 enhances the phagocytotic activity in the injured spinal cord. A–C: Phagocytosis, indicated by LAMP2 expression, was increased by MR16-1-treatment. D–H: Quantification of the LAMP2$^+$ inflammatory subsets in injured chimeric mice indicated that the microglia had significantly higher phagocytotic activity than the hematogenous macrophages. MR16-1-treatment did not affect the phagocytotic activity of either cell subpopulation. Values are means ± SEM. *$P<0.05$. Scale bars = 200 μm in A, B; 20 μm in D–G.

cytokines or neurotrophic factors, and since previous reports show that the inhibition of IL-6 signaling drastically alters the expression profiles of various cytokines (Matsumura et al., 1999; Romano et al., 1997), the temporary inhibition of IL-6 signaling may, by altering the chemical milieu, underlie the shift in the dominant inflammatory cell type following MR16-1 treatment.

Given the characteristics of hematogenous macrophages vs. those of resident microglia, the MR16-1-induced switch in the central player in post-SCI inflammation should be beneficial. The evidence bears out this prediction. In the injured spinal cord, broad destruction of the blood–spinal cord barrier (BSCB) permits the infiltration of hematogenous macrophages into the lesion. If the infiltrating neutrophils and macrophages are depleted or blocked, tissue sparing improves, as does axonal regeneration/sprouting (Gris et al., 2004; Popovich et al., 1999; Saville et al., 2004). The cytotoxicity of hematogenous macrophages may be due to their increased NO production in the injured CNS (Ponomarev et al., 2007). In addition, a recent report showed that direct physical interactions between activated hematogenous macrophages and axons causes the axons to retract; microglia have a similar effect, but it is much weaker (Horn et al., 2008).

Despite the detrimental effects of hematogenous macrophages, the accumulation of inflammatory cells is considered to be critical for the repair process, because these cells clear away tissue debris and release neurotrophic factors. Previous studies demonstrated that the resident microglia play an active role in repairing the injured CNS, through their relatively high phagocytotic activity (Schilling et al., 2005) and by releasing various neuroprotective cytokines or neurotrophic factors (Lalancette-Hebert et al., 2007; Lambertsen et al., 2009). In fact, the tissue debris within the injured spinal cord contains myelin-derived axonal growth inhibitory factors (Bregman et al., 1995; Merkler et al., 2001) that hinder the repair process after SCI, so clearing away this debris is prerequisite for axonal re-growth.

In this study, MR16-1 treatment led to an increased accumulation of microglia, which expressed higher levels of the phagocytic markers LAMP2 and Mac2 than did the hematogenous macrophages. Furthermore, the Oil red O-stained intracellular area of microglial cells was greater than that of hematogenous macrophages. These data indicate that the microglia had higher phagocytotic activity than the hematogenous macrophages, and this activity was enhanced by the MR16-1 treatment.

The enhanced phagocytosis by MR16-1 treatment, along with attenuation of injury, resulted in decreased Oil red O staining (indicating reduced deposition of myelin) and decreased immunostaining for the axonal growth inhibitor Nogo-A, at the chronic phase of post-SCI inflammation. These effects could have contributed to the formation of a permissive environment for the regeneration or sprouting of neuronal fibers. In fact, the process of spinal cord repair seemed to be enhanced, given the increase in the RT-97$^+$ fibers and 5HT$^+$ serotonergic fibers between 14 and 42 dpi. The higher density of RT-97 fibers in the penumbral area in the treated group, and the lack of RT-97+ fibers at the center of the injury site in both groups, may indicate that enhanced sprouting contributed to the increase in 5HT+ fibers caudal to the lesion site (Supplemental Fig. 2).

Taken together, it is possible that the immediate administration of MR16-1 affected only the late phase of inflammation, because the change in cytokine profile by MR16-1 enhanced the participation of microglia in the inflammatory process, resulting in a tissue-protective inflammation. Our results with LFB, Oil red O, and immunostaining for